Electron Probe Micro-Analysis of gas bubbles in solids: a novel approach.

by M.Verwerft,
Reactor Materials Research Department, SCK•CEN, Boeretang 200, B-2400 Mol, Belgium

Abstract

The local analysis of retained noble gas in nuclear fuel is inherently difficult since the physical form under which it is stored varies from atomically dispersed to bubbles with a diameter of several hundreds of nm. One of the techniques that has been applied since more than twenty years is Electron Microprobe Analysis (EPMA). Although many important results were obtained with this technique, its application to the analysis of highly inhomogeneous materials is limited. The EPMA technique indeed is difficult to apply to samples that are not homogeneous on the scale of the electron-solid interaction volume. In this paper, a method is developed to analyse a system of gas bubbles distributed in a solid matrix. It is based on multiple voltage EPMA measurements combined with a Scanning Electron Microscopic analysis of the bubble size distribution.

1. Introduction

The rising costs associated with either long term storage or reprocessing of spent nuclear fuel compel nuclear power management to increase the average fuel burnup. With increasing burnup, a high amount of fission products is also accumulated in the fuel matrix. One particular class of fission products are the noble gases xenon and krypton. They have a high fission yield and tend to escape from the matrix as they are insolubile in either UO_2 or MOX. At low operating temperatures, the mobility is limited and the noble gas atoms are believed to remain atomically dispersed. With increasing temperature, the gas atoms form bubbles of increasing diameter both at intragranular and intergranular sites, and a fraction escapes to the free volume of the fuel rod. Important information on the fission gas behaviour is obtained from retained gas concentration profiles of individual pellets. Although several analysis methods have been applied to study the fission gas behaviour, if entire cross section analysis with subgrain resolution is needed, only EPMA can provide the necessary information. In this paper, we will focus on the problems of electron microprobe analysis of gas bubbles in a solid.

2. Electron Probe Analysis of Xe.

2.1 Experimental setup.

The Xe profiles were acquired with a CAMEBAX-R Microbeam adapted for the analysis of radioactive samples. It is run under the XMAS controlling software of SAMx. Its spectrometers are internally shielded to reduce background due to the high gamma activity of irradiated fuel. Analyses are performed with high probe currents (typically 50nA to 200nA), and the analysers are operated in differential mode. It is possible to obtain acceptable detection limits even on highly active samples.

When analysing the Xe concentration on cross section samples from rods that have been subjected to high linear power regimes, one always observes a pronounced concentration drop at the centre (figure 1). The release of volatile fission products is a well-known phenomenon, and when one measures the composition of the gas in the free volume of a fuel rod, Xe is indeed found. On basis of Xe-profiles such as represented in figure 1, one may in principle calculate the amount of released gas and compare the result with a direct analysis of the gas contained in the rod's free volume. If one does as such for the present fuel rod, one obtains on basis of EPMA measurements an estimated release of Xe of more than 50%, while the direct measurement shows a release of only 4%. Other microanalysis methods also indicate that electron microprobe analyses systematically underestimate the true retained gas content. This of course limits the applicability of the method to fission gas analysis. For reasons cited in the introduction, EPMA results are still widely used and it is therefore interesting to investigate in detail the problem of this systematic underestimation.

2.2 Multiple voltage analyses

In general, one chooses the accelerating voltage such as to minimise correction factors, and in general an overvoltage ratio between 2 and 3 is recommended. Light element analyses are accordingly performed at much lower accelerating voltages (3kV to 5kV) than standard analyses (15kV to 25kV). In nuclear fuel, one is usually concerned with characteristic lines of energies between 2kV and 6kV, in which case an accelerating voltage of 10kV to 15kV would in theory yield best results. If however one would perform the same analysis at different accelerating voltages, one expects identical result apart from minor deviations due to the limited accuracy of X-ray correction models. For the present samples, this is not the case however. In figure 2, three Xe profiles are reproduced, which are all acquired exactly along the same path, but at different accelerating voltages: 10kV, 15kV and 30kV.

At radial positions $\frac{r}{r_0} \geq 0.75$ (r_0 = pellet radius), the apparent Xe concentration is independent from the accelerating voltage. At positions $\frac{r}{r_0} \leq 0.5$, the Xe concentration approaches zero, again irrespective of the experimental conditions. In the transition zone however, the apparent Xe concentration largely depends upon the applied accelerating voltage: the higher the applied potential, the higher the measured Xe concentration. The difference between an analysis performed at 30kV and one performed at 10kV is maximal at relative radius $\frac{r}{r_0} = 0.65$ and amounts to more than 50%.

Qualitatively, one may understand this by looking at the difference between SEM images acquired at different applied voltages. At low accelerating voltages (figure 3a), only those bubbles are visible which intersect with the free surface, at higher voltages on the other hand (figure 3b), one also observes sub-surface bubbles. Since the bubbles that intersect with the free surface obviously do not contain any Xe, there is a concentration gradient between the very surface where the Xe content is zero and depths larger than the bubble diameter, where the average Xe concentration remains constant. Since at higher accelerating voltages, one probes the concentration deeper into the material, it is clear that increasing the accelerating voltage will result in a higher apparent Xe concentration. A quantitative analysis of such a structure however is less straightforward.

2.3 X-ray correction procedure for a bubble distribution

The system we are dealing with, is that of a polydispersed system of spheres filled with a noble gas mixture at high pressure in a ceramic matrix (figure 4a). Apart from the gas spheres, numerous other precipitates are present in the UO_2 matrix, and a number of elements remain atomically dissolved. We will however consider only the gas filled spheres and the UO_2 matrix, the other effects are considered as higher order disturbances.

Conventional quantitative electron microprobe analysis is limited to samples which are homogeneous at the scale of the electron-solid interaction volume. This interaction volume depends on the applied acceleration voltage and the density of the sample. Recently, the analysis of layered structures (2D homogeneous systems) has become possible by EPMA techniques at least to a certain extent. There exist however no universal technique to analyse systems which are truly inhomogeneous in three dimensions.

It is not the X-ray signal of a point analysis close to a single bubble that is of interest, but the statistical average of a zone with a specific bubble distribution. Experimental electron probe analyses of such a bubble distribution are therefore generally performed with a defocussed beam in order to average the signal over a substantial volume of material. In the usual case of normal electron beam incidence, one needs to consider the average concentration variations along the normal direction. The structure will thus further be simplified (figure 4b) in order to implement it in an X-ray correction code.

In order to describe the structure properly, one also has to include its intersection with the free surface. Since in an EPMA experiment one does not probe the bulk but rather the surface down to a depth of a few µm, it is the intersection with the free surface that will govern the measured X-ray intensity. To account for the influence of the free surface, one must calculate the X-ray intensity for all possible intersection configurations (figure 5, middle and right). In practice, the number of different configurations that is considered (typically a few hundred), is determined by the accuracy that is aimed at.

The intersection with a free surface has the consequence that any bubble which is cut by the free surface no longer contains Xe (figure 5, middle). Taking into account that the sample preparation involves grinding and polishing, which damages the top layer, Xe will also be lost from bubbles which are entirely closed, but which intersect with the damaged zone. If the bubbles are moreover at high pressure, they can only remain intact if the covering layer is strong enough to counteract the internal pressure. To account for these effects, a parameter δ is introduced, which expresses the thickness of the depleted layer.

For each configuration, the emerging X-ray intensities of uranium, oxygen and xenon is calculated and the result is averaged:

$$I_\alpha = \frac{1}{N_{conf}} \sum_{i=0}^{N_{conf}} f_\alpha(\rho_i(z)) \qquad \alpha = U, O, Xe \qquad (1)$$

In this expression, $f_\alpha(\rho_i(z))$ is the calculated K-ratio for the considered element of each configuration. These calculated X-ray intensities (expressed as K-ratios) are used as input to determine the apparent Xe concentration for a given bubble distribution.

Essential to a correct calculation of the X-ray intensities of an inhomogeneous sample, is the use of a model that correctly describes the depth distribution of the generated primary X-rays. The conventional ZAF methods which were based on the depth distribution profile of Philibert (1964), provide satisfactory results for homogeneous samples with weak absorption effects. For samples which are inhomogeneous in depth, or in which absorption is very important, such as for light element analysis, the ZAF corrections are not appropriate since the profiles calculated on basis of the Philibert model are too crude a representation of the true depth distribution of primary X-rays. The evolving requirements in materials research necessitating e.g. the analysis of light elements in a heavily absorbing matrix and the characterisation of multilayer systems has led in the eighties to the development of more advanced depth distribution models. The latter methods are often referred to as the 'phi-rho-z' models. Several researchers (Packwood and Brown, 1980; Tanuma and Nagashima, 1983; Love et al., 1984; Bastin et al., 1986; Pouchou and Pichoir, 1984a, b) have developed models that improve on the Philibert approach. These X-ray depth profile models were then incorporated (often by the same authors) in commercial X-ray correction codes. Unfortunately, the commercially available X-ray correction codes do not provide the necessary flexibility to calculate a system as the one described above. For the actual problem, we have chosen the parabolic PAP method (Pouchou and Pichoir, 1991).

We have implemented the hypothetic 1D layer structure with the following variables:

- density of the matrix (ρ_{fuel})
- bubble diameter (<D>)
- bubble volume fraction (V_V)
- number of configurations (N_c)
- density of the gas (ρ_{gas})
- thickness of the depleted top layer (δ)

The calculations are performed using the theoretical value for the density of UO_2 (ρ_{fuel} = 10,96g/cm^3). The local bubble diameter <D> and the porosity volume fraction V_V are determined by SEM observations. The number of configurations (N_c) is imposed by convergence criteria. For a known concentration of gas and bubble volume fraction, the gas density may in theory be calculated using the equation of state of noble gases Xe and Kr at elevated pressures. The gas concentration however is the unknown parameter and must thus be calculated iteratively. The parameter δ is estimated on basis of a comparison of X-ray intensities acquired at different acceleration voltages. Typical calculated results are shown in figure 6.

3. Comparison of calculated and experimental Xe profiles

In order to perform quantitative calculations, one must introduce the true values of the bubble size distribution as a function of the radial position. In particular, one has to determine the average diameter <D> and the bubble volume fraction V_V.

In figure 7, the experimental Xe profiles are compared to calculated ones in the assumption of total retention. The calculated curves are generally in good agreement with the experimental data series for the three applied accelerating voltages. Systematic deviations are however observed at radial positions $0.750 > r/r_0 > 0.675$ and at positions $0.600 > r/r_0$.

In the zone $0.750 > r/r_0 > 0.675$, the calculated concentrations systematically underestimate the measured values. This might be due to the presence of a bubble population fraction which is invisible in a SEM analysis. The observed bubble volume fraction indeed is too low to accomodate all gas at pressures below that of solid Xe. Other studies also have shown that in the early stage of bubble growth, only a fraction of the bubbles coarsen, while another fraction stays at the (sub-)nm scale. In such a case, the present calculations fail since only the size distribution of the bubbles that are visible by SEM observations, is taken into account.

In the zone $0.600 < r/r_0$, the calculations systematically overestimate the experimental results, which indicates release of intragranular Xe. It should be stressed that the EPMA results do not allow one to determine towards which sinks the Xe diffuses (grain boundaries, grain boundary bubbles, intrergranular pores, ...). This has to be assessed by e.g. systematic SEM observations. Those observations indeed show a distinct change in intragranular porosity at the point where massive fission gas release starts.

4. Conclusions and summary

Electron probe microanalysis probes the surface rather than the bulk concentrations. In this specific case of analysing gas bubbles in a solid, a concentration gradient exists due to sample preparation. If this influence on the apparent gas concentration is neglected, large errors are made. In order to account for this, we have performed model calculations. The parameters of this model are either directly determined by SEM observations, or adjusted through a full exploitation of multiple voltage analyses. The advantage of performing analyses of the same area but at different voltages lies in the fact that one can judge the validity of the model itself. In this particular case, we have extensively used the multiple voltage analyses to separate the geometry related effects on the X-ray signal from the decrease due to bulk release.

The most important result that can be obtained from the present analysis, is the determination of the point at which true gas release occurs. If one would e.g. interpret the 15kV data directly, one would have to accomodate a fission gas release as high as 30% in a structure where intergranular bubbles are still closed and represent only a very small fraction of the total bubble volume fraction. This would mean that one has to accept the possibility that gas is stored at very high pressures on grain boundaries and in grain boundary bubbles. After correction for the influence of the geometry on the apparent Xe concentration, one may conclude that massive gas release from the bulk of the grains occurs with the simultaneous development of large, interconnected pores which may directly vent to the pre-existing intergranular pores.

References

J.L. Pouchou and F. Pichoir, J. de Physique, 45 C2, 17 (1984).
J.L. Pouchou and F. Pichoir, J. de Physique, 45 C2, 47 (1984).
J.L. Pouchou and F. Pichoir, in *Electron Probe Quantitation*, ed K.F.J. Heinrich and D.E. Newbury (Plenum, New York, 1991) p. 31.
C. Ronchi and C.T. Walker, J. Phys. D 13, 2175 (1980).
R.H. Packwood and J.D. Brown, *Microbeam analysis-1980* ed. D.B. Wittry (San Fransisco Press, San Fransisco, 1980)
S. Tanuma and K. Nagashima, Mikrichim. Acta, 1, 299 (1983).
G. Love, D.A. Sewell and V.D. Scott, J. de Physique, 45 C2, 21 (1984).

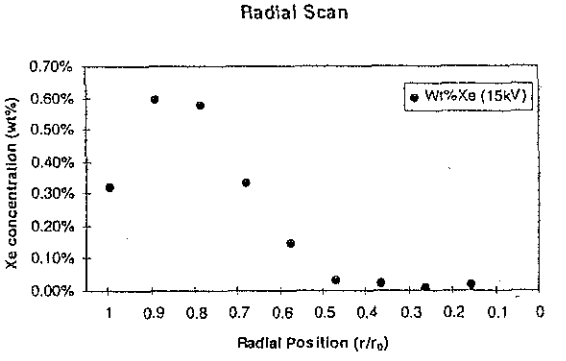

Figure 1 Xe concentration variation as a function of radial position. The electron beam accelerating voltage was chosen as 15kV.

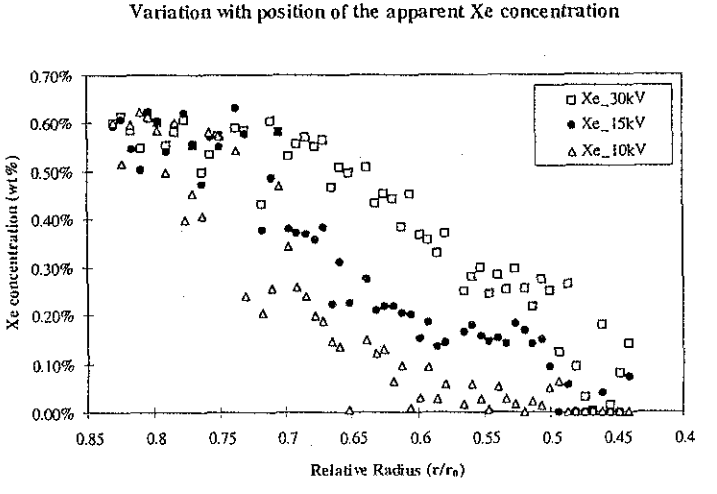

Figure 2. Variation in apparent Xe concentration as a function of radial position for different accelerating voltages. The drop of Xe concentration occurs first for the lower accelerating voltages.

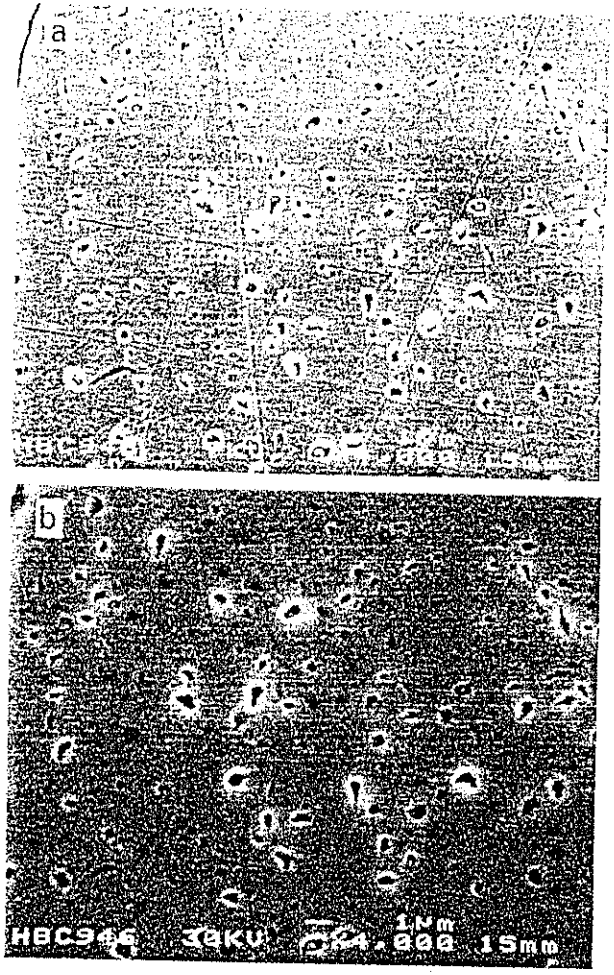

Figure 3. SEM images of an identical zone, but imaged at different accelerating voltages: (a) 7kV, (b) 30kV. The sub-surface, Xe-filled bubbles are only visible at higher accelerating voltage.

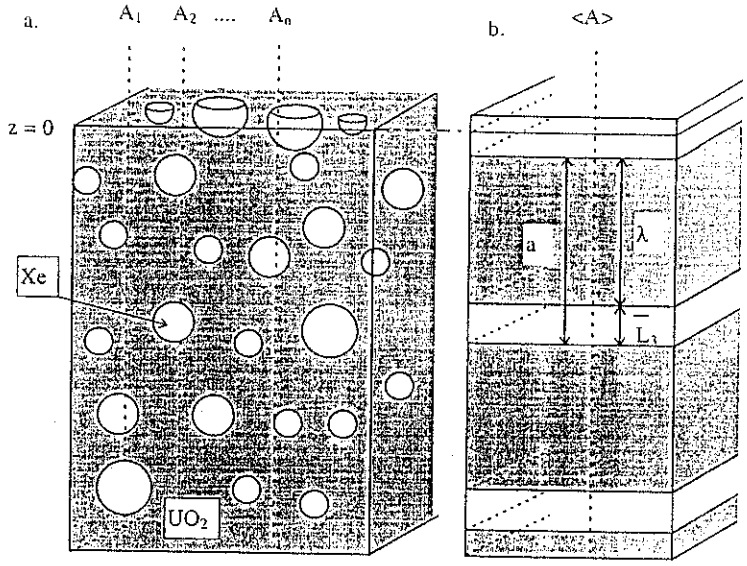

Figure 4. a. Schematic representation of the bubble configuration: the ceramic matrix is dark grey, closed bubbles are light grey and open bubbles are white. The free surface is at depth z = 0.
b. Average linear intersection, with a schematic representation of the linear parameters $\overline{L_3}$ and λ, and the repeat period a.

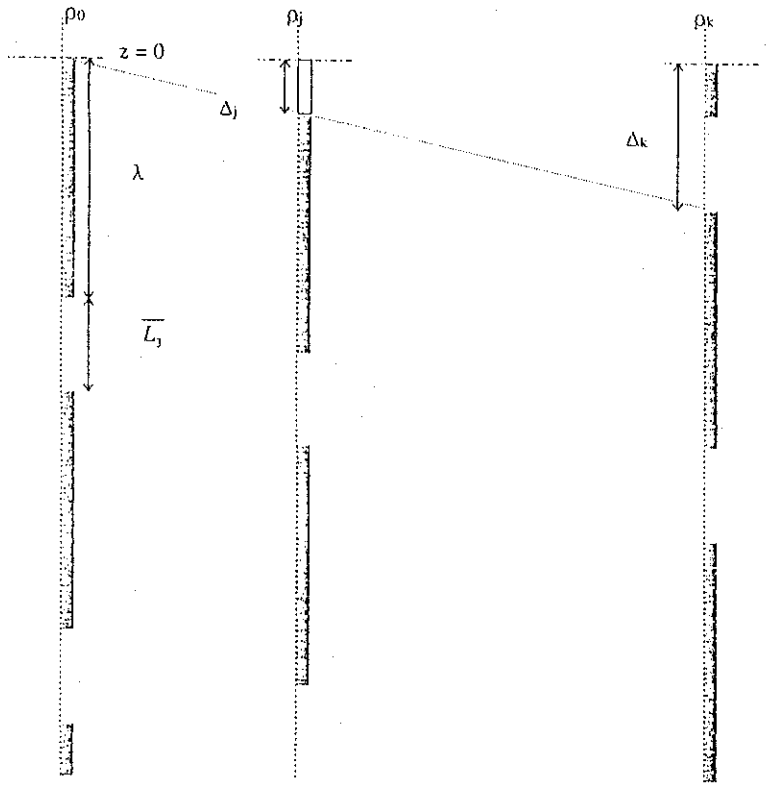

Figure 5. Three different configurations of the same 1D representation of a bubble distribution.

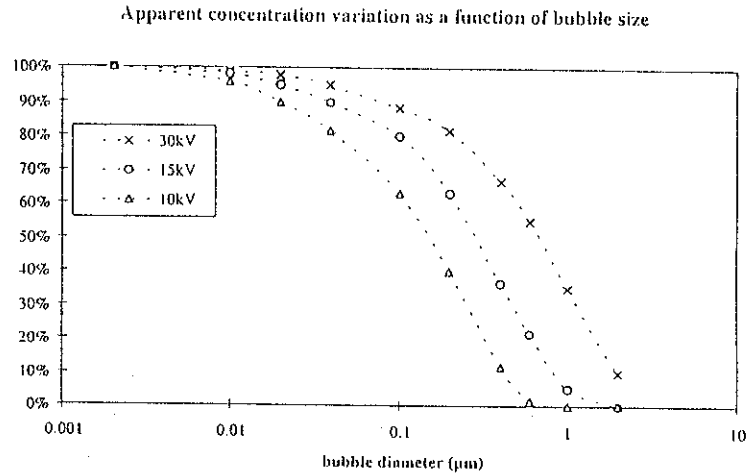

Figure 6. Calculation of the apparent Xe concentrations as a function of bubble diameter. The absolute concentrations are plotted against the left axis, and the difference is plotted against the right axis.

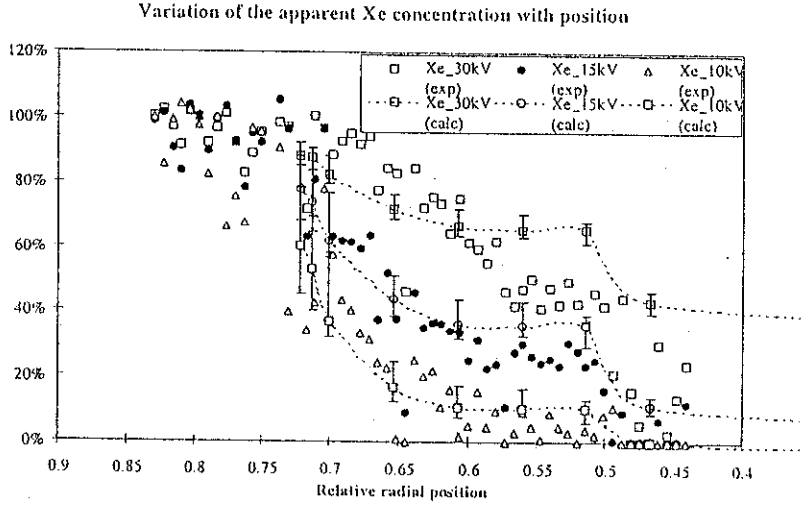

Figure 7 Comparison between experimental and calculated Xe profiles.

EPMA of gas bubbles in solids: a novel approach

M. Verwerft
Reactor Materials Research
SCK•CEN

EPMA of Gas Bubbles in Solids

- Introduction
  - Goal: Xe distribution profiles
  - Why EPMA ? - What's the problem ?
- SEM of bubble distributions
- Quantifying X-ray corrections for a bubble distribution
- Experimental vs. calculated results
- Conclusions

Introduction

- Nuclear fuel accumulates ~6000ppm noble gases (Xe & Kr) at 5At% burnup.
- Their retention & release are important for fuel behaviour modelling (mechanical & thermal).
- Distribution profiles of entire cross sections (10mm ϕ) with subgrain resolution ← EPMA (WDS)

Introduction

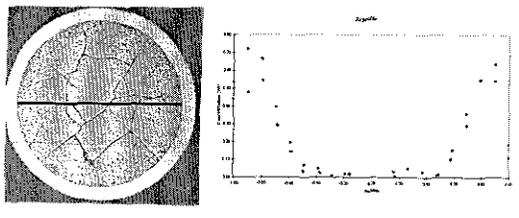

Apparent Xe concentration across a pellet diameter.

Introduction

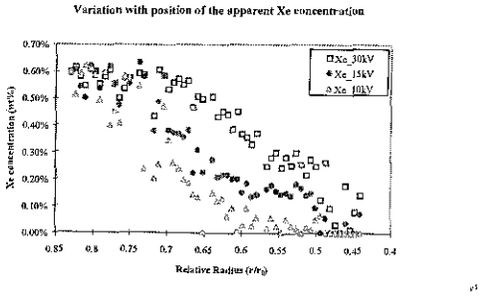

SEM of Bubble Distributions

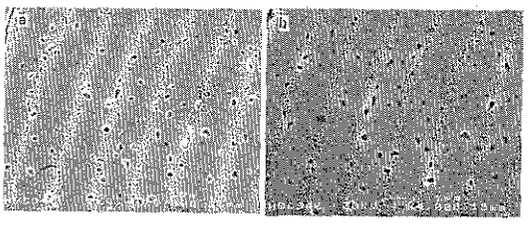

Influence of the accelerating voltage: (a) 7kV, (b) 30kV

SEM of Bubble Distributions

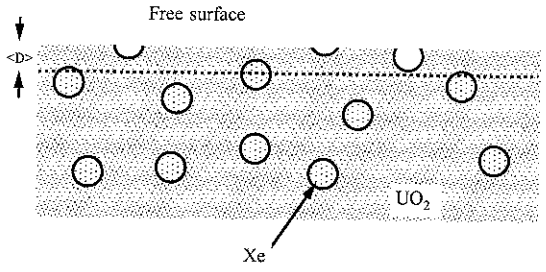

SEM of Bubble Distributions

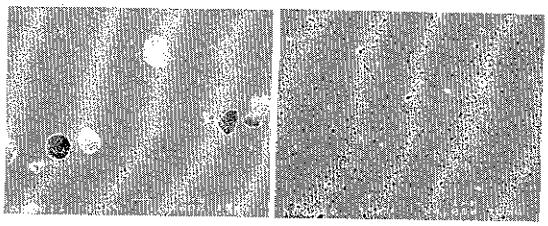

Bubble distribution at relative radius r/r_0 = 0.69

(a) low mag, (b) high mag

SEM of Bubble Distributions

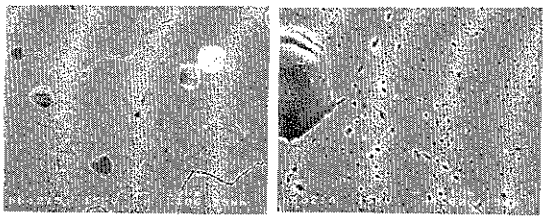

Bubble distribution at relative radius r/r_0 = 0.65

(a) low mag, (b) high mag

SEM of Bubble Distributions

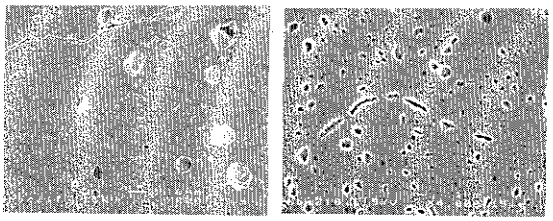

Bubble distribution at relative radius r/r_0 = 0.55

(a) low mag, (b) high mag

SEM of Bubble Distributions

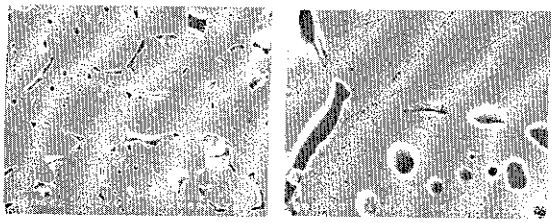

Bubble distribution at relative radius r/r_0 = 0.10

(a) low mag, (b) high mag

SEM of Bubble Distributions

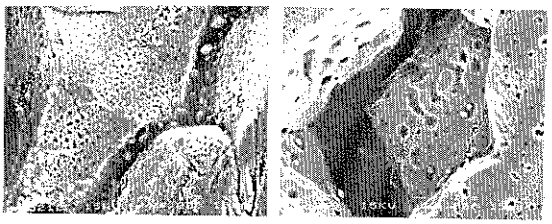

Bubble distribution on grain boundaries: (a) at relative radius r/r_0 = 0.69, (b) at relative radius r/r_0 = 0.54.

X-ray correction for a bubble distribution

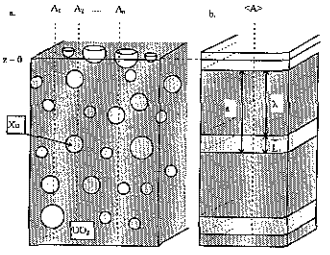

Mean intercept length: $\overline{L_3} = \frac{2}{3} < D >$

Mean free edge-to edge distance: $\lambda = \frac{2}{3} < D > \left(\frac{1 - V_V}{V_V} \right)$

X-ray correction for a bubble distribution

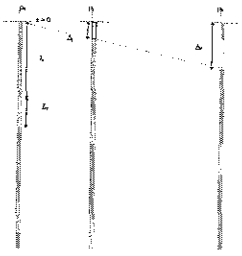

Three different intersection configurations for the same average 1D structure.

X-ray correction for a bubble distribution

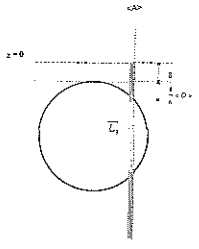

The topmost position of an intact Xe bubble depends on surface damage and bubble pressure.

X-ray correction for a bubble distribution

- Construct an equivalent 1D structure on basis of the mean intercept length (λ) and mean free edge-to-edge distance (L_3):

$$\rho_0(z) = \sum_n \Re(z - n.a) \text{ with } a = \lambda + L_3 \text{ and } n = \text{integer}$$

$$\Re(\xi) = \rho_{UO_2} \qquad 0 < \xi \leq \lambda$$
$$= \rho_{Xe} \qquad \lambda < \xi \leq a$$
$$= 0 \qquad \text{elsewhere}$$

X-ray correction for a bubble distribution

- Calculate all possible intersection configurations:

$$\rho_i(z) = \rho_0(z - \Delta_i) \qquad \text{with} \qquad \Delta_i = \frac{i.a}{N_c}$$

$$\rho_{Xe} = 0 \quad \text{for} \quad z \leq \Delta_i \quad \text{and} \quad \Delta_i \leq \overline{L_3} + h = \frac{5}{4}.\overline{L_3} + \delta$$

X-ray correction for a bubble distribution

- Calculate the k-ratio for each configuration and take the average:

$$I_\alpha = \frac{1}{N_c} \sum_{i=0}^{N_c} f_\alpha(\rho_i(z)) \qquad \alpha = \text{U, O, Xe}$$

X-ray correction for a bubble distribution

- Implementation in parabolic PAP model, with parameters:
  - density of the matrix (ρ_{fuel}) — literature
  - bubble diameter (<D>) — SEM
  - bubble volume fraction (V_V) — SEM
  - number of configurations (N_c) — convergence
  - density of the gas (ρ_{Xe}) — "no release"
  - thickness depleted top layer (δ) — conc. ratios

X-ray correction for a bubble distribution

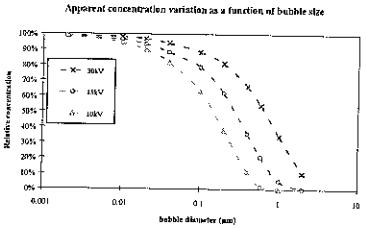

X-ray correction for a bubble distribution

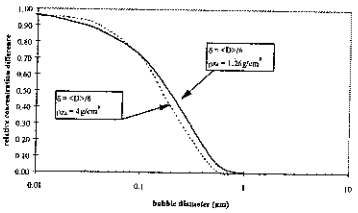

The gas density ρ_{Xe} has little influence on the model.

X-ray correction for a bubble distribution

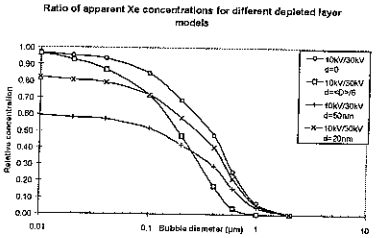

The depleted layer thickness has major influence on the model.

Experiment vs. model calculations

- Fit the parameter δ to the ratio of apparent concentrations as measured at different accelerating voltages.
- Compare calculated and experimental "apparent Xe concentration profiles" for different accelerating voltages.

Experiment vs. model calculations

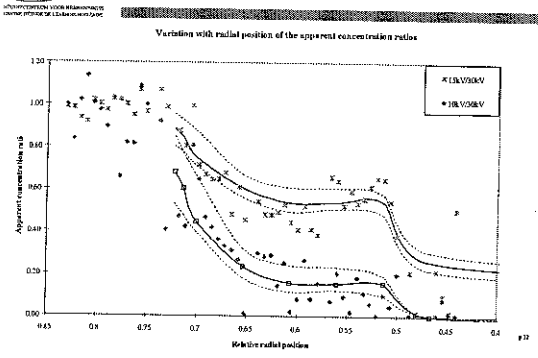

Experiment vs. model calculations

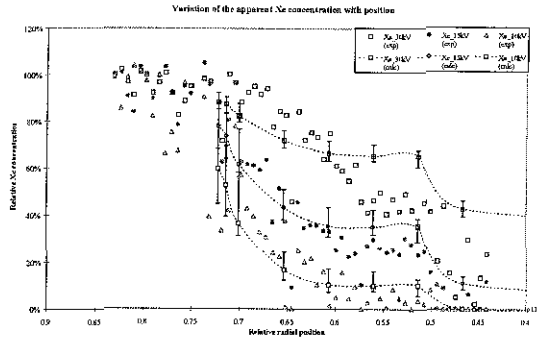

Conclusions: specific

- In the zone $0.750 > r/r_0 > 0.675$, the calculated concentrations slightly underestimate the measured values:
  SEM observations do not reveal small bubbles
- In the zone $0.600 < r/r_0$, the calculations systematically overestimate the experimental results :
  release of intragranular Xe
- No evidence for huge quantities of retained Xe on grain boundaries.

Conclusions: general

- EDS & WDS probes the surface, not the bulk: be careful when analysing surface concentration gradients.
- An independent validation of the model is provided by multiple voltage analyses.
- True 3D correction does not yet exist
- Implementing your own X-ray package really is fun! (and sometimes necessary)